

Development of Thin-Junction Detector

W. Chen, G. Carini, J. Keister, Z. Li, and P. Rehak, *Fellow, IEEE*

Abstract—Two methods to produce a thin-junction sensor are reported here. The first method consists of a regular boron implantation with energies of 2 keV (dose of $1 \times 10^{15}/\text{cm}^2$) and 5 keV (dose of $1 \times 10^{14}/\text{cm}^2$) into silicon directly, and 10 keV ($1 \times 10^{14}/\text{cm}^2$), 45 keV ($1 \times 10^{15}/\text{cm}^2$) into Si through a thin oxide layer (500 Å and 1000 Å respectively) to form a junction. An aluminum layer was coated in the same vacuum system after back-sputtering to remove oxide on top of the implanted silicon substrate. This method may have the following advantages: 1) it may improve the soft X-ray radiation hardness of the device because there is no oxide layer on the junction; 2) it substantially attenuates the incident visible light; and 3) it allows detection of low energy X-ray down to 300 eV. The second method consists of a low energy of 2 keV and dose of $1 \times 10^{15}/\text{cm}^2$ boron implantation into the bare silicon followed by laser annealing that activates boron with minimal diffusion, to retain the ultra thin-junction. The laser annealing method was compared with control wafers. Two of the control wafers were implanted by boron with the same energy and dose as that of the laser annealed wafer. One of them was annealed using high temperature of 1000°C and time of 30 minutes thermal annealing. The other was annealed using our regular annealing temperature of 700°C and with longer annealing time of 17 hours. The remaining control wafer was implanted by boron with higher energy of 45 keV and dose of $1 \times 10^{15}/\text{cm}^2$ (our standard boron implantation energy and dose) and annealed using regular (700°C, 30 min) thermal annealing.

Index Terms—Dead-layer, detectors, implementations, laser-annealing, silicon-dioxide, thin-junction.

I. INTRODUCTION

THIS paper is a preliminary work to obtain the fabrication parameters for the production of silicon drift detectors (SDD). These detectors are going to be used as the prototypes to perform analysis of the elements on the Moon surface by X-ray fluorescence. The fluorescence of the lunar surface is due to the Solar wind. The shining part of the Moon is the one that emits the fluorescence X-ray. The system is under design in the Marshall Space Flight Center (MSFC) for a potential NASA Lunar Mission. The entire X-ray spectroscopic system will be located on a moon satellite. This spectroscopic system consists of an array of collimators defining a sensitive area swiping the Moon surface. The X-ray collimators are followed by an array of SDD connected by low noise electronics. They provide 1) the energy of individual X-rays for the identification of the elements and 2) the time information of the X-ray detection to assign the location of the emitting source on the Moon surface from the

known trajectory of the satellite. One of the most important elements to detect is carbon, whose K_{α} energy is 282 eV. This presents two main challenges for the system. 1) The equivalent noise charge (ENC) of the read-out electronics chain following individual SDD should be below 10 e, for better detection of the carbon 282 eV line. 2) The entrance window for X-ray detection should be transparent to X-rays and at the same time must stop almost completely the moonlight caused by the illumination of the Moon surface by the Sun. Detailed studies of the light absorption and reflection showed that a 110 nm thick layer of aluminum covering the X-ray entrance window can sufficiently attenuate the visible light to a level that will induce the current below the leakage current of the SDD. The silicon following this aluminum layer should ideally be fully efficient starting from the surface. Any realistic implantation would produce a certain depth of junction which would lead to a certain depth of dead layer. In this work we are trying to find the optimal processing parameters to make the junction as thin as possible and make the dead layer as thin as possible using existing techniques.

II. SIMULATION AND RESULTS

We are using SILVACO simulation tools. Its ATHENA enables us to simulate the fabrication of the devices by using various parameters to get the corresponding desirable devices. Its ATLAS allows us to simulate the devices' characteristics by applying the bias to the devices that we constructed by using ATHENA.

The simulation parameters we chose consist of using boron implant into silicon directly or into Si through a thin oxide layer to form a junction. The substrate is $n < 111 >$, resistivity of 4–6 k Ω -cm and thickness of 300 μm silicon. The device structure is $p^+/n/n^+$ with the X-ray entrance window on the p^+ -side. In the simulations, the implantation energies vary from 2 keV to 45 keV, and the corresponding doses are: for 2 keV, $1 \times 10^{15}/\text{cm}^2$; for 5 keV, $1 \times 10^{14}/\text{cm}^2$; for 10 keV, $1 \times 10^{14}/\text{cm}^2$; for 25 keV, $1 \times 10^{15}/\text{cm}^2$; and for 45 keV, $1 \times 10^{15}/\text{cm}^2$. The annealing temperatures vary from 700°C to 1000°C, and the annealing times vary from 30 min to 17 hr.

In Fig. 1, the simulation results from the SILVACO show the potential distribution near the silicon surface in the silicon bulk when an appropriate reverse bias of 5 V is applied on the detector. Fig. 1(a) indicates the result simulated from directly implanting boron into silicon. Fig. 1(b) indicates the result simulated from implanting boron into Si through a thin layer of silicon dioxide. The potential distributions are quite different in these two cases. In Fig. 1(a) we mark a number of depths to demonstrate the complexity of the dead layer corresponding to the junction. t_m indicates the minimum potential depth from the silicon surface. t_f is defined as the full collection depth, since beyond this depth the electrons will be fully collected; and t_0 is defined as the zero collection depth, since none of the electrons generated in this depth is going to be collected. The dif-

Manuscript received January 18, 2007; revised June 27, 2007. This work was supported in part by the U.S. Department of Energy under Contract DE-AC02-98CH10886.

The authors are with the Brookhaven National Laboratory, Upton, NY 11973 USA (e-mail: weichen@bnl.gov; carini@bnl.gov; jkeister@bnl.gov; zhengl@bnl.gov; rehak@bnl.gov).

Color versions of one or more of the figures in this paper are available online at <http://ieeexplore.ieee.org>.

Digital Object Identifier 10.1109/TNS.2007.905173

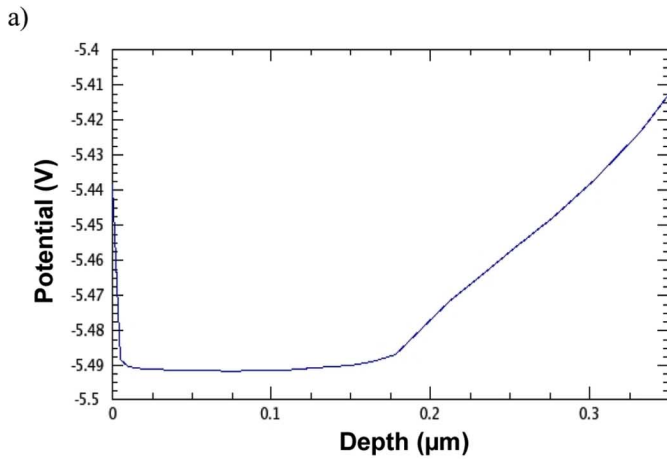
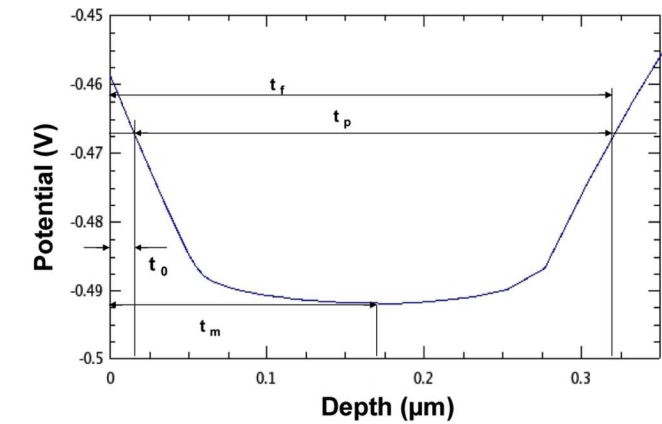


Fig. 1. The potential distribution results in the silicon bulk produced by SILVACO simulation. (a) is the result simulated by implantation of 45 keV, $1 \times 10^{15}/\text{cm}^2$ Boron into silicon directly. (b) is the result simulated by implantation of the same energy and dose of Boron into Si through 1000 Å oxide layer. Both of them annealed at 700°C for 30 min.

ference $t_p = t_f - t_0$ is defined as the partial collection depth, where some electrons generated in this region will be collected, depending on where exactly they are located in that region. If the electrons are generated near the left hand side within the t_p region, most of them will be swept toward the surface of the silicon and thus not collected by the signal of the detector. If the electrons are generated near the right hand side within the t_p region, most of them will be swept toward the inner part of the bulk of silicon and collected by the anode of the detector. The difference between the potentials corresponding to t_p and t_m is equal to the thermal energy kt/q , which is about 25 mV.

In Fig. 2, we plot the dead layer depth obtained from SILVACO simulation versus the implantation energies. We can see that the dead layer t_m in the case of implanting boron into Si through silicon dioxide is thinner than the one in the case of implanting boron directly into silicon. The oxide thicknesses corresponding to each implant are: for 10 keV, 500 Å; for 25 keV, 1000 Å; and for 45 keV, 1000 Å. For energy below 5 keV, the oxide thickness has to be thinner than 500 Å. Oxide of such thickness cannot be determined with the naked eye by its color. Therefore we do not use oxide for such a low energy implant. We can also see that as the implantation energy decreases, the dead layer depths for these two cases converge to the thinner depth.

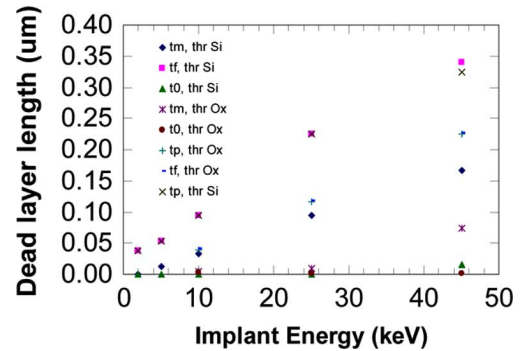


Fig. 2. The simulation results show the dead layer depths as a function of the implantation energies in the cases of implanting into Si through oxide and directly into silicon followed by annealing at 700°C for 30 min.

We also developed a total charge collection simulation for a completely fabricated device in order to detect the carbon K_α line, which is completely independent of SILVACO simulation. The simulation results are shown in Fig. 3(a) In the left hand side curve, when t_p is 20 nm, the charge densities collected at below 20 e and around 70 e are similar; therefore, in the right hand side curve, the total charge collection has a dominant peak at the carbon K_α line. In the left hand side curve of Fig. 3(b), when t_p is 90 nm, the charge density collected at below 20 e becomes higher than that around 70 e; therefore, in the right hand side curve, the tail of the total charge collection becomes higher. In the left hand side curve of Fig. 3(c), when t_p is 180 nm, the density of charge collected at below 20 e is even higher than that around 70 e; therefore, in the right hand side curve, the tail of the total charge collection becomes even higher. In the left hand side curve of Fig. 3(d), when t_p is 260 nm, the charge density been collected at below 20 e is much higher than that around 70 e; therefore the tail of the total charge collection curve becomes the dominant one. In other words, if t_p increases as the shape of the potential distribution changes, we will lose the sensitivity for the carbon K_α line detection. We notice the influence of t_p to the total charge collection by looking from Fig. 3(a) through (d). As t_p increases, the percentage of lost charges increases, therefore the tail of the total charge collection curve rises. In the case where $t_p = 260$ nm, the carbon K_α line is not a dominant peak any more, and we are losing the sensitivity for the carbon K_α line detection. Therefore the collection efficiency is not only influenced by the depth of the “fully dead layer”, but even more by the depth of the partially collecting layer t_p . In the experimental part of this contribution, we have the means to detect only the t_m rather than the full set of all depth parameters. Therefore we have to rely on the results of SILVACO simulations to establish process parameters to produce an optimal entrance window.

III. FABRICATION

In order to simplify the process of the investigation, we are currently fabricating simple square-shaped diodes instead of silicon drift detectors. Their areas are 25 mm² and 10 mm². The diodes are surrounded by a guard ring as shown in Fig. 4.

We used two methods to produce a thin-junction sensor. The first method consists of using regular boron implant, with energies of 5 keV ($1 \times 10^{14}/\text{cm}^2$) into silicon directly, and 10 keV

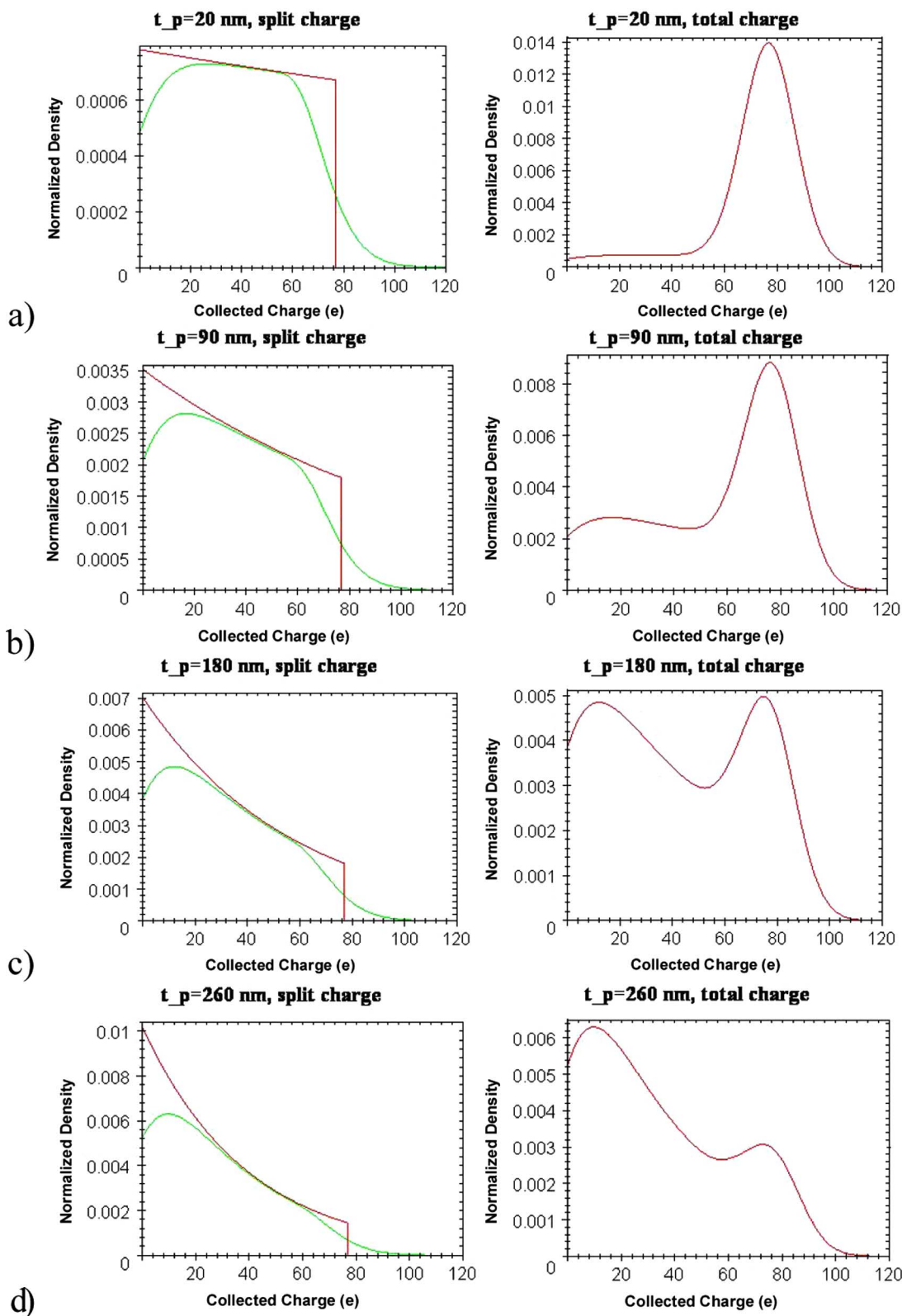


Fig. 3. The simulation results show how the split depth t_p influences the shape of the total charge collection. (a) When t_p is 20 nm, the charge densities collected at below 20 e and around 70 e are similar; therefore the total charge collection curve has a dominant peak at the carbon k_{α} line. (b) When t_p is 90 nm, the charge density collected at below 20 e becomes higher than around 70 e; therefore the tail of the total charge collection curve becomes higher. (c) When t_p is 180 nm, the density of charge collected at below 20 e is even higher than around 70 e; therefore the tail of the total charge collection curve becomes even higher. (d) When t_p is 260 nm, the charge density been collected at below 20 e is much higher than around 70 e; therefore the tail of the total charge collection curve becomes the dominant one.

($1 \times 10^{14}/\text{cm}^2$), 45 keV ($1 \times 10^{15}/\text{cm}^2$) into Si through 500 Å and 1000 Å thin oxide layers respectively to form a junction.

A 110 nm thick layer of aluminum covering the X-ray entrance window has been proposed to sufficiently block the visible light

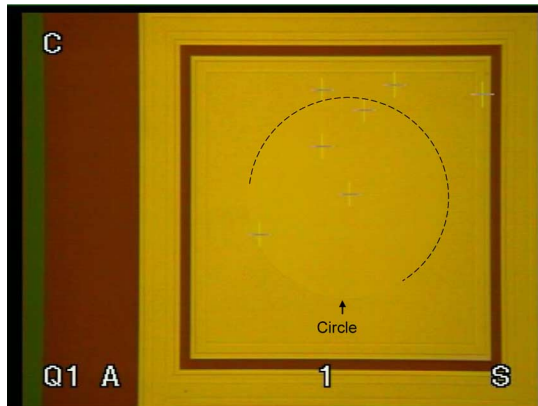


Fig. 4. The shape of the diode used in the study. 110 nm aluminum coating is done only in the center circle, while outside the circle much thicker aluminum is coated in order to be bonded without destroying the junction.

and the radiation next to the visible light. We have upgraded our aluminum deposition system by adding a new back sputtering feature to remove the native oxide before sputtering aluminum within the same vacuum. The aluminum layer was coated in the same vacuum system after back-sputtering to remove native oxide on top of silicon substrate. This method may have the following advantages: 1) it improves the soft X-ray radiation hardness of the device that is caused by the lack of oxide layer on the junction; 2) it absorbs the visible light; and 3) it allows the detection of low energy X-rays down to 300 eV. This 110 nm aluminum coating is done only in the center circle (Fig. 4, one can barely see it, so we marked a part of it with a dashed line), while outside the circle much thicker aluminum is coated in order to be bonded without destroying the junction. Since the current design of the diode makes it impossible to test the light attenuation and the rest of the study is mostly about the forming of the thin junction, we decided to cover the entire square area of the diode with 180 nm aluminum for the remaining sample diodes. In this way the aluminum can be bonded easily without destroying the diode and the fabrication process can be simplified.

The annealing of ion-implanted silicon is an integral part of the detector fabrication. The annealing process should result in minimum diffusion of doped atoms while obtaining an excellent removal of defects and a very high degree of doping activation. The inadequacy of conventional furnace annealing has led researchers to investigate alternative methods to furnace annealing based on lasers, electron beams, lamps, resistance heaters and ion-beam annealing technologies. Out of the various alternative techniques mentioned above, the laser annealing is the most promising one in terms of producing ultra-thin junction [1]–[5]. The use of laser annealing on a low energy ion implanted junction is our second method in producing a thin junction sensor with minimum dead layer. This method uses a 248 nm excimer-laser annealing (700 mJ/cm²) to activate low energy of 2 keV and dose of 1×10^{15} /cm² boron implantation that produces an ultra-thin junction. The laser annealing method was compared with control wafers. Two of the control wafers were implanted by boron with the same energy as that of laser annealed wafer. One of them was annealed using high temperature (1000°C, 30 min) thermal annealing. The other was an-

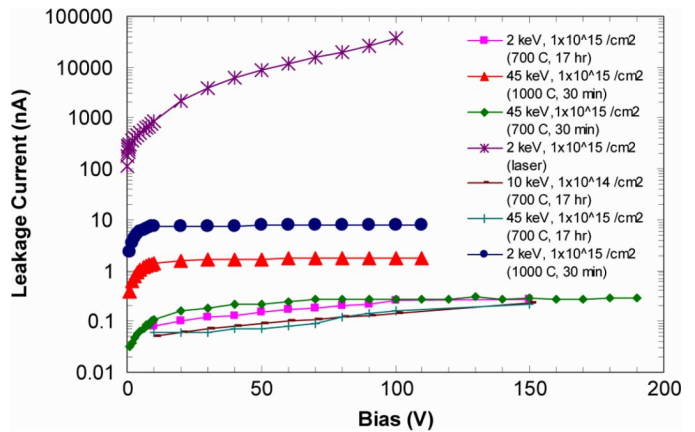


Fig. 5. The leakage current measured as a function of bias voltage for the diodes (all of them are 0.1 cm² in size) produced by various fabrication parameters. The thickness of the wafer is 400 μ m.

nealed using our regular annealing temperature (700°C) with longer annealing time (17 hrs). The remaining control wafer is implanted by boron with higher energy of 45 keV and dose of 1×10^{15} /cm² (our standard boron implantation) and annealed using regular (700°C, 30 min) thermal annealing. Laser annealing was done at AMBP Tech Corporation in Piscataway, NJ. The laser is Lambda Physk Compex 102. The laser wavelength is 248 nm, the pulse duration is 25 ns, and the repetition rate is 10 Hz.

IV. TEST RESULTS AND DISCUSSION

Fig. 5 shows the leakage current test results from the diodes that were fabricated by the method we mentioned in the previous section. The top curve (highest leakage current) is the one produced by laser annealing. We were surprised by this high leakage current result. The second highest leakage current curve is the one produced by implantation energy identical to the laser annealed one (2 keV, 1×10^{15} /cm²) but annealed at a higher temperature, 1000°C for 30 min. The third highest leakage current curve is the one produced by a 45 keV implantation energy with 1×10^{15} /cm² dose and annealed at a higher temperature, 1000°C, for 30 min. The remaining curves in Fig. 5 are in the pA range. These are much better diodes, because they underwent the regular annealing temperature (700°C) in 30 min and in 17 hours. The 17 hours time produced better results because more defects were annealed out. For all practical purpose, a time of 30 min is sufficient enough. Fig. 6 shows the leakage current of the diodes produced by longer annealing time, but implanted by a different energy. The data is identical to the data from the three lowest curves of Fig. 5. The 10 keV (1×10^{14} /cm²) and 45 keV (1×10^{15} /cm²) implants are all implanted into Si through oxide layers of 500 Å and 1000 Å respectively. They yield very similar results. The slightly higher leakage current curve is the one produced by a 2 keV (1×10^{15} /cm²) implantation into Si without the thin oxide layer. The lower implantation energy should produce a thinner junction. However implanting into Si through a thin oxide layer seems to change the potential distribution shape as analyzed in the simulation section, and therefore produces a thinner dead layer which further influences the leakage current. It seems that if the implant dose and the annealing condition

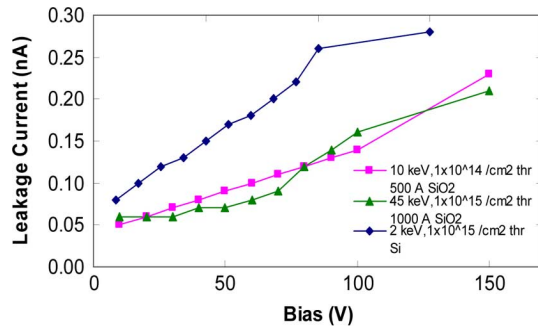


Fig. 6. The leakage current measured as a function of the bias voltage for the diodes (0.1 cm^2) produced by various Boron implantation energies and annealed under identical conditions at 700°C for 17 hr. The thickness of the wafer is $400 \mu\text{m}$. The data is identical to the data from the three lowest curves of Fig. 5.

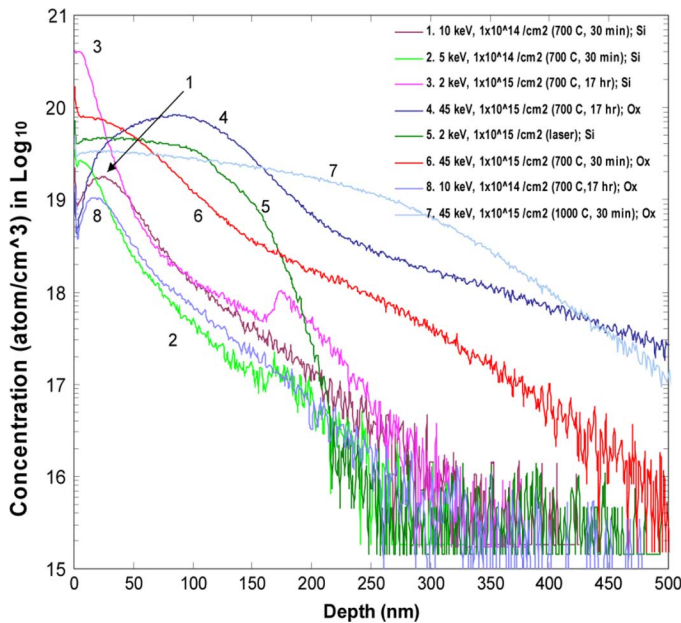


Fig. 7. SIMS test results of diodes showing the Boron doping versus the depth of silicon profile with various implantations and annealing method. The substrate is n-type silicon with doping density about $10^{12}/\text{cm}^3$.

are constant, one may always select a low enough energy and implant through a thin enough oxide layer, and this process produces a thin dead layer. However in reality an oxide of thickness less than 500 \AA cannot be determined by its visible color, and therefore the choice of energy is limited by the capability of producing a measurable and uniformly thin silicon dioxide.

We sent some sample-diodes to do the Second Ion Mass Spectroscopy (SIMS) test. The aluminum contact layers have been removed for those samples prior to SIMS. The SIMS test results are shown in Fig. 7. One can observe different diode implantation profiles corresponding to implantation energies for different diodes. The diode with 2 keV ($1 \times 10^{15}/\text{cm}^2$) implant, the diode with 10 keV ($1 \times 10^{14}/\text{cm}^2$) implant and the diode with 45 keV ($1 \times 10^{15}/\text{cm}^2$) implant have profiles corresponding to the respective implantation energies. Surprisingly the profile of the diode with laser annealed is completely unlike a 2 keV ($1 \times 10^{15}/\text{cm}^2$) implant profile. A possible explanation is the laser annealing energy we were using, $700 \text{ mJ}/\text{cm}^2$, was not right and that could drive the doped atoms too deep into the silicon, making the resulting profile look like the 45 keV

TABLE I
FABRICATION PARAMETERS OF SAMPLES FOR DC CURRENT TEST ARE LISTED

Impl	2 keV	5 keV	10 keV	10 keV	45 keV
Dose ($/\text{cm}^2$)	1×10^{15}	1×10^{14}	1×10^{14}	1×10^{14}	1×10^{15}
Anneal	700°C 17 h	700°C 30 m	700°C 30 m	700°C 17 h	700°C 17 h
Al (\AA)	1800	1800	1800	1800	1800
Back Sputr	No	Yes	Yes	No	No
Impl Thru	Si	Si	Si	500 \AA SiO ₂	1000 \AA SiO ₂

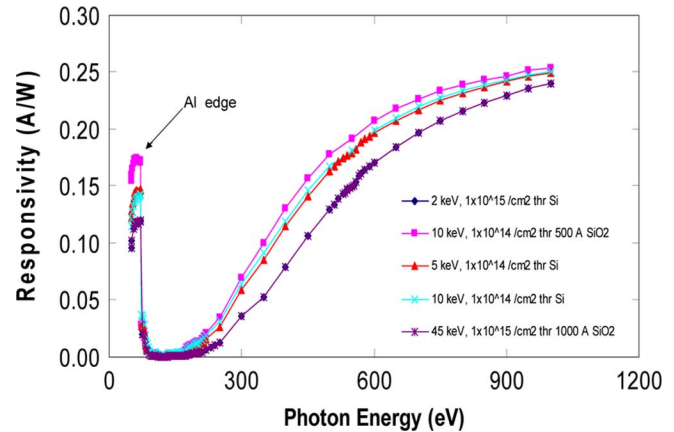


Fig. 8. The DC current measurement with X-ray energy ranging from 50 eV to 1 keV.

($1 \times 10^{15}/\text{cm}^2$) implant profile. Therefore the laser annealed sample did not give us a conclusive result. Further investigation is needed. From SIMS result, it showed that the diode with 10 keV ($1 \times 10^{14}/\text{cm}^2$) implant into Si through 500 \AA SiO₂ has thinner junction than the diode with 10 keV ($1 \times 10^{14}/\text{cm}^2$) implant into Si directly.

We chose five diodes, whose fabrication parameters are listed in Table I, for the DC current measurement in the National Synchrotron Light Source's (NSLS) UV beam line U3C [6] at the Brookhaven National Laboratory. This beam line is used for absolute radiometric calibration in the 50 to 1000 eV X-ray range [7].

Fig. 8 shows the absolute responsivity calibration (DC current) measurement result. The X-ray energy used here ranges from 50 eV to 1 keV. The aluminum L edge is apparent at 73 eV. At higher photon energies the responsivity approaches the theoretical maximum of 0.27 A/W , which is W_{Si}^{-1} , where W_{Si} is the mean electron-hole pair production energy in silicon (3.66 eV [8]). However one can hardly see the oxygen peak at 534 eV. This is because our diode's active area of $400 \mu\text{m}$ thick silicon is covered with 1800 \AA of aluminum. The native silicon dioxide in between them is very small (estimated $30\text{--}50 \text{ \AA}$) by comparison. Therefore this method cannot detect the existence of the native silicon dioxide which was left in between the aluminum and silicon substrate. The DC current versus the implantation energy corresponding to different X-ray energy is plotted in Fig. 9. It shows that the diodes with 10 keV implantation energy and $1 \times 10^{14}/\text{cm}^2$ dose are the most efficient ones. By fitting the curves in Fig. 8, we obtain the dead layer depths listed

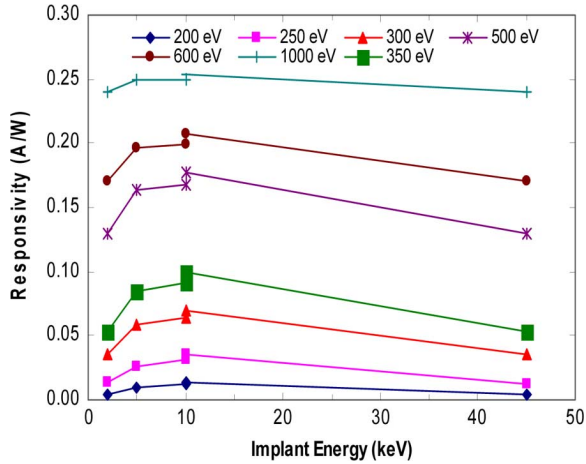


Fig. 9. The efficiencies of the diodes correspond to their implantation energies at various X-ray energies.

TABLE II
DEAD LAYER DEPTHS OBTAINED BY FITTING THE CURVES IN FIG. 8 ARE LISTED HERE

Impl (keV)	Dose (/cm ²)	Annealing	Back Sputter	t _{Si} (dead) (Å)	Al (Å)
45 (1000 SiO ₂)	1x10 ¹⁵	700 °C, 17 h	N	1560	1800
10 (500 SiO ₂)	1x10 ¹⁴	700 °C, 17 h	N	182	1800
2	1x10 ¹⁵	700 °C, 17 h	N	1560	1800
5	1x10 ¹⁴	700 °C, 30 min	Y	533	1800
10	1x10 ¹⁴	700 °C, 30 min	Y	332	1800

in Table II for various fabrication parameters. In the fitting, we assume the aluminum thickness is known (1800 Å), and neglect the aluminum oxide on the aluminum surface. We assume all the oxide layer is the native silicon dioxide. The fitting function of the responsivity $S(E)$ can be written as:

$$S(E) = W_{Si}^{-1} \cdot \left(e^{-t_{Al}/\lambda_{Al}(E)} \cdot e^{-t_{Si}/\lambda_{Si}(E)} \cdot e^{-t_{SiO_2}/\lambda_{SiO_2}(E)} \right) \quad (1)$$

where t_{Al} , t_{Si} , t_{Ox} are the fitting parameters. W_{Si} is 3.66 eV [8], $\lambda_{Al}(E)$, $\lambda_{Si}(E)$, $\lambda_{SiO_2}(E)$ (above 150 eV) come from [9] and $\lambda_{SiO_2}(E)$ (50–150 eV) comes from [10]. Fig. 10 shows the fitting of the experiment data where the dots are the experimental data and the smooth line is the fitting. The trend of the experimental results is in agreement with the simulated results. The diode with 10 keV, $1 \times 10^{14}/\text{cm}^2$ Boron implanting into Si through 500 Å SiO₂ has the thinnest dead layer, about 18 nm, and is the most efficient diode in the group. Its dead layer is thinner than the junction depth which comes from the SIMS measurement shown in Fig. 7. This sample produces a thin junction and a thin dead layer, although their thicknesses are not equal. The dead layer we measured in this DC experiment is t_m , which had been defined in the simulation section.

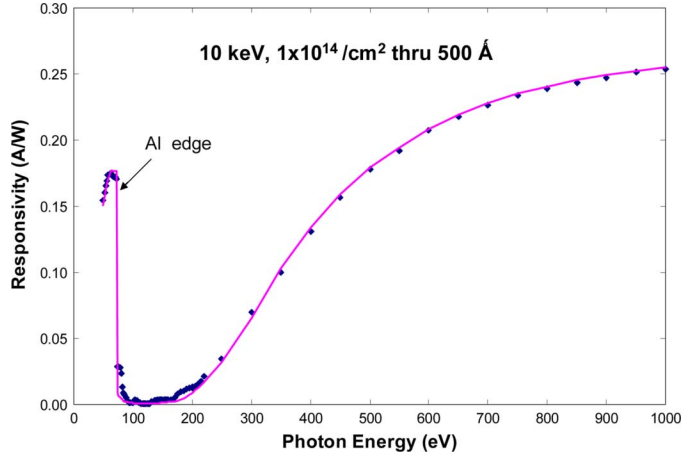


Fig. 10. Fitting to the experimental data is shown. The dots are the experimental data, and the smooth line is the fitting.

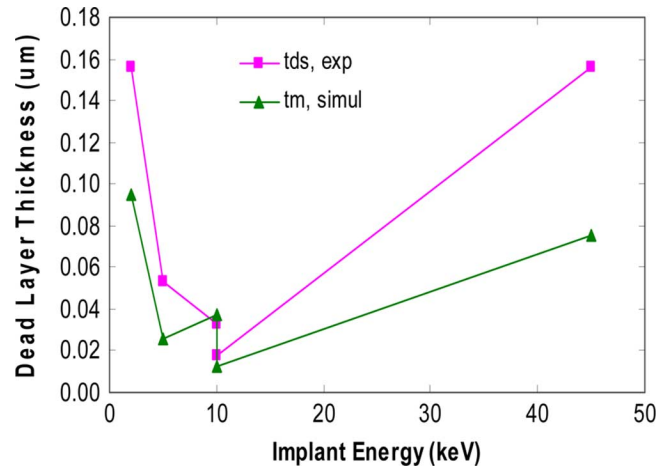


Fig. 11. The dead layer thickness versus the implantation energies: a comparison of the experimental with the simulation results.

V. CONCLUSION

In this work we showed that by implanting into Si through silicon dioxide and lowering the implantation energy, we can improve the junction thickness and the dead layer depth. The choice of the implantation energy is limited by the capability of producing a measurable and uniformly thin silicon dioxide. Although annealing at 700°C for a long time gives a low leakage current, a time of 30 min is sufficient. We choose a 10 keV ($1 \times 10^{14}/\text{cm}^2$) implantation into Si through a 500 Å silicon dioxide and an annealing at 700°C for 30 min (with Back-Sputtering to remove native silicon dioxide) as our recipe for SDD fabrication for the planned NASA Lunar mission. In this experiment, we cannot detect any native silicon dioxide layer left between the aluminum layer and the silicon substrate. We observed a reasonable agreement between the measured and simulated dead layer depth t_m . We are confident that we can rely on SILVACO simulation to produce an optimal entrance window within our constraints. The laser annealing method failed to give a conclusive result. Further investigation is needed.

ACKNOWLEDGMENT

The authors would like to thank R. Beuttenmuller for his support during the DC current experiment.

REFERENCES

- [1] G. Fortunato, L. Mariucci, M. Stanizzi, V. Privitera, S. Whelan, C. Spinella, G. Mannino, M. Italia, C. Bongiorno, and A. Mittiga, "Ultra-shallow junction formation by excimer laser annealing and low energy (<1 keV) B implantation: A two-dimensional analysis," *Nucl. Instrum. Methods Phys. Res. B*, vol. B186, pp. 401–408, 2002.
- [2] J. Narayan, O. W. Holland, W. H. Christie, and J. J. Wortman, "Rapid thermal and pulsed laser annealing of boron fluoride-implanted silicon," *J. Appl. Phys.*, vol. 57, p. 2709, 1985.
- [3] V. Privitera, C. Spinella, G. Fortunato, and L. Mariucci, "Two-dimensional delineation of ultra shallow junctions obtained by ion implantation and excimer laser annealing," *Appl. Phys. Lett.*, vol. 77, p. 552, 2000.
- [4] A. G. Cullis, H. C. Webber, and N. G. Chew, "Correlation of the structure and electrical properties of ion-implanted and laser-annealed silicon," *Appl. Phys. Lett.*, vol. 36, p. 547, 1980.
- [5] Y. F. Chong, K. L. Pey, A. T. Wee, A. See, L. Chan, Y. F. Lu, W. D. Song, and L. H. Chua, "Annealing of ultra shallow p⁺/n junction by 248 nm excimer laser and rapid thermal processing with different preamorphization depths," *Appl. Phys. Lett.*, vol. 76, p. 3197, 2000.
- [6] Brookhaven National Laboratory, Upton, NY [Online]. Available: <http://www.bnl.gov/u3cx8a> and/or <http://www.nsls.bnl.gov/beam-lines/beamline.asp?blid=U3C>
- [7] R. J. Bartlett *et al.*, "Characteristics and performance of the Los Alamos VUV beam line at the NSLS," *Nucl. Instrum. Methods Phys. Res. A*, vol. A266, p. 199, 1988.
- [8] F. Scholze, H. Rabus, and G. Ulm, "Mean energy required to produce an electron-hole pair in silicon for photons of energies between 50 and 1500 eV," *J. Appl. Phys.*, vol. 84, p. 2926, 1998.
- [9] B. L. Henke, E. M. Gullikson, and J. C. Davis, "X-ray interactions: Photo absorption, scattering, transmission, and reflection at E = 50 – 30000 eV, Z = 1–92," *Atomic Data Nucl. Data Tables* vol. 54, no. 2, pp. 181–342, 1993 [Online]. Available: http://www.cxro.lbl.gov/optical_constants
- [10] J. Rife and J. Osantowski, "Extreme ultraviolet optical properties of two SiO₂ based low-expansion materials," *J. Opt. Soc. Amer.*, vol. 70, p. 1513, 1980.